Electrophysiological Analysis of Cloned Cyclic Nucleotide-Gated Ion Channels[1]

Qiang Leng[2], Richard W. Mercier, Bao-Guang Hua, Hillel Fromm, and Gerald A. Berkowitz*

Department of Plant Science, University of Connecticut, Storrs, Connecticut 06269–4067 (Q.L., R.W.M., B.-G.H., G.A.B.); and Centre for Plant Sciences, Leeds Institute for Biotechnology and Agriculture, School of Biology, University of Leeds, Leeds LS2 9JT, United Kingdom (H.F.)

Electrophysiological studies were conducted on the cloned plant cyclic nucleotide-gated ion channels AtCNGC2 and AtCNGC1 from Arabidopsis, and NtCBP4 from tobacco (*Nicotiana tobacum*). The nucleotide coding sequences for these proteins were expressed in *Xenopus laevis* oocytes or HEK 293 cells. Channel characteristics were evaluated using voltage clamp analysis of currents in the presence of cAMP. AtCNGC2 was demonstrated to conduct K^+ and other monovalent cations, but exclude Na^+; this conductivity profile is unique for any ion channel not possessing the amino acid sequence found in the selectivity filter of K^+-selective ion channels. Application of cAMP evoked currents in membrane patches of oocytes injected with AtCNGC2 cRNA. Direct activation of the channel by cyclic nucleotide, demonstrated by application of cyclic nucleotide to patches of membranes expressing such channels, is a hallmark characteristic of this ion channel family. Voltage clamp studies (two-electrode configuration) demonstrated that AtCNGC1 and NtCBP4 are also cyclic nucleotide-gated channels. Addition of a lipophilic analog of cAMP to the perfusion bath of oocytes injected with NtCBP4 and AtCNGC1 cRNAs induced inward rectified, noninactivating K^+ currents.

Cyclic nucleotide-gated nonselective cation channels (cngcs) represent a newly identified family of plant ion transport proteins (Köhler et al., 1999; Leng et al., 1999). This putative family of plant ion channels shares deduced secondary and tertiary structural homology with a diverse family of cngcs cloned and characterized from animal systems (Zagotta and Siegelbaum, 1996). However, primary amino acid sequence homology between this family of plant proteins and their presumed animal homologs is not very great (approximately 22%; Leng et al., 1999).

Animal cngcs are primarily, but not in all cases (Lee et al., 2001), expressed in sensory neurons and function in signal transduction systems. However, cngcs have been detected in cell types other than sensory receptor neurons, and have been cloned from a number of different tissue types in animals (Biel et al., 1999b; Finn et al., 1996; Lang et al., 2000), suggesting that their role in multicellular organisms may be more diverse than originally thought. Animal cngcs are characterized by the following functional parameters: They are not, or only weakly, voltage gated; they are activated by direct binding of cyclic nucleotide (cAMP and cGMP); they are selective for cations but do not discriminate between conductance of cations such as Ca^{2+}, Na^+, and K^+; their activation by cyclic nucleotides is blocked by calmodulin; and they show varying degrees of conductance rectification (Zagotta and Siegelbaum, 1996). It is interesting that their relative conductance of specific cations, their relative activation by cAMP versus cGMP, and the extent of their conductance rectification are typically related to the specific role they play in a diverse number of signal transduction pathways and, in addition, other physiological processes in animals.

Genome sequence analysis suggests that at least in Arabidopsis, this group of proteins may contain the greatest number (20) of individual members of any plant ion channel family (Maser et al., 2001); the Glu receptor family of putative plant ion channels (Lacombe et al., 2001) may also have 20 members. However, the diverse range of roles they play in plant function is only currently being elucidated. Initial reports suggested a role (similar to that of animal cngcs) in signal transduction. Clough et al. (2000) found that Arabidopsis plants with a mutation in the gene (*dnd1*) encoding the plant cngc AtCNGC2 did not display a hypersensitive response (apoptosis) upon pathogen infection. Other work (Köhler et al., 2001) supports the conclusion of Clough et al. (2000) that AtCNGC2 may play a general role in programmed cell death. Demonstration of protein-protein interactions between plant cngcs and the cytosolic secondary signaling molecule calmodulin (Schuurink et al., 1998; Arazi et al., 2000; Köhler and Neuhaus, 2000), and a functional interaction between plant cngcs and the cytosolic secondary messengers

[2] Present address: Yale School of Medicine, Department of Cellular and Molecular Physiology, 333 Cedar Street, B121–SHM, New Haven, CT 06520.

* Corresponding author; e-mail gerald.berkowitz@uconn.edu; fax 860–486–0682.

Ca^{2+}, cAMP, and cGMP (Leng et al., 1999), further supported a role for these channels in plant signal transduction pathways. However, current work in a number of laboratories (Sunkar et al., 2000; Maathuis and Sanders, 2001; White, 2001; I.N. Talke, N. Bouche, D. Bouchez, H. Fromm, D. Sanders, and F.J.M. Maathuis, personal communication; C.W.M. Chan, J.F. Harper, and M.R. Sussman, personal communication[3]) has presented preliminary evidence that cngcs may provide a physiologically significant pathway for cation uptake from the rhizosphere. These studies suggest that, in this role, some individual cngcs may impact plant response to soil salinity and heavy metals. Thus, an evolving picture has emerged that indicates that cngcs may be involved, in manners not yet characterized, in a broad array of mechanisms impacting plant growth, development, and response to environmental stresses.

Despite the paucity of information about the specific roles cngcs play in plant response to external signals, growth, and development, even less is known about the functional properties of plant cngcs. Of the 20 individual members of the protein family, only AtCNGC2 has been functionally characterized as an ion channel (Leng et al., 1999). As is the case with most ion channel proteins, the conductance and regulatory parameters of plant cngcs may be related to their physiological roles in planta. An important research imperative, therefore, is the expression of cloned plant cngcs in heterologous systems, which allow for electrophysiological analysis of the recombinant proteins. In this report, our previous initial voltage clamp analysis of the plant cngc AtCNGC2 (Leng et al., 1999) is extended, and preliminary evidence is presented documenting the channel characteristics of some other members of this protein family.

RESULTS AND DISCUSSION

Cation Selectivity

Prior work from this laboratory (Leng et al., 1999) provided initial functional characterization of AtCNGC2 as a ligand (cyclic nucleotide)-gated ion channel by expression of the protein in *Xenopus laevis* oocytes. Two-electrode voltage clamp recordings of oocytes injected with AtCNGC2 cRNA displayed (cAMP and cGMP dependent) maximal K^+ (96 mM bath [KCl]) currents of approximately 1-μA amplitude at hyperpolarizing (-160 mV) command voltages. In the experiment shown in Figure 1, similar cAMP-dependent K^+ currents were observed. In addition, AtCNGC2 was found to conduct other monovalent cations (Li^+, Cs^+, and Rb^+) to an extent nearly
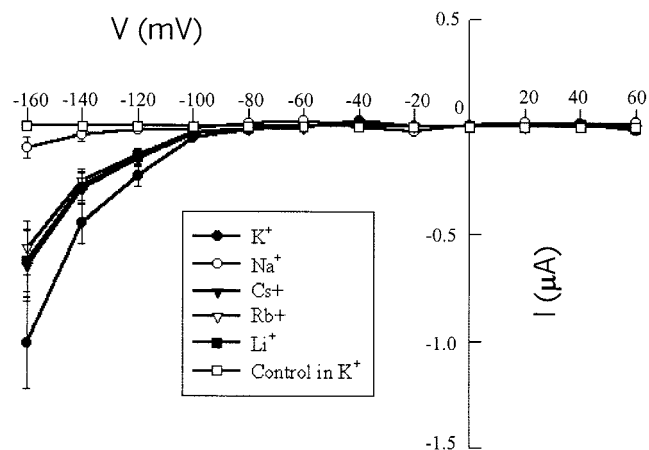
Figure 1. Current/voltage relationship of AtCNGC2 currents recorded from oocytes (two-electrode configuration) with a range of monovalent cations in the perfusion bath. All currents (except for the control) are presented as leak subtracted recordings. Command voltages were applied in 20-mV steps between +60 and −160 mV. For each monovalent cation shown, currents were recorded with a bath solution lacking dibutyryl-cAMP. cAMP-activated currents were recorded after 40 min perfusion with dibutyryl-cAMP. In each case, the leak current was subtracted from the cAMP-activated current, yielding the current values shown at each command voltage tested. The control treatment was recorded with KCl and dibutyryl-cAMP in the bath. Current values are presented as means ($n = 6$ [control], 11 [K^+], 8 [Na^+], 7 [Cs^+], 6 [Rb^+], and 4 [Li^+]) $\pm$ SE.

as great as K^+ (in the presence of cAMP), whereas Na^+ currents were much lower. cAMP-dependent Na^+ currents recorded from oocytes injected with AtCNGC2 cRNA were not much greater than those recorded from water-injected oocytes. Relative conductivity of a recombinant channel expressed in oocytes can only be estimated when recordings are made in the two-electrode configuration; the volume of the oocyte is too large to allow for equilibration with the contents of the electrode pipette solution, so only the cation concentrations outside the oocyte can be known with certainty. However, we estimated relative permeability of AtCNGC2 to monovalent cations in the experiment shown in Figure 1 following the approach used by Schachtman et al. (1992). Using this approach (current values used were measured at the end of a 1.6-s pulse at a command potential of -160 mV), relative conductance values (K^+ is 100, measured on 11 oocytes) are (values given as means $\pm$ SE followed by oocyte number): Na^+, 10 ± 5 (8); Cs^+, 64 ± 16 (7); Rb^+, 56 ± 126; and Li^+, 62 ± 14(4). Using this same approach, the relative permeability of the K^+-selective channel KAT1 for Na^+ was calculated by Schachtman et al. (1992) to be 7 ± 8; a value not significantly different from the relative Na^+ permeability we calculate here for AtCNGC2. Considering that the K^+ content of oocytes is typically at least 10-fold greater than the ambient Na^+ content (Weber, 1999), the relative Na^+ permeability calculated from these values is certainly an overestimation. With respect to the strong selectivity

shown for K^+ over Na^+ conductance, the channel properties of AtCNGC2 are unlike any known cyclic nucleotide-gated channels cloned to date. As mentioned previously, the animal cngcs cloned and functionally characterized using voltage clamp analysis do not discriminate between Na^+ and K^+.

The amino acid sequence of the channel pore region and the helix of the flanking S6 membrane-spanning region for a number of K^+ channels, animal cngcs, and plant cngcs is portrayed in Figure 2. K^+-selective channels have the amino acid triplet "GYG" motif in the selectivity filter within the ion-conducting pore of the channel (Fig. 2); this has been demonstrated to be the basis for the strong discrimination against Na^+ conduction by these channels (Heginbotham et al., 1994; Doyle et al., 1998). Analysis of the deduced amino acid sequences of cloned animal cngcs has noted that this critical GYG motif within the selectivity filter of the pore is absent, and that this is the likely basis for Na^+ conduction by cngcs (Finn et al., 1996; Zagotta and Siegelbaum, 1996). Although AtCNGC2 lacks the GYG triplet within the selectivity filter also, the amino acids within this pore motif of AtCNGC2 differ from the corresponding amino acid triplet of animal cngcs (Fig. 2). It also should be noted that the amino acid residues within the selectivity filter of AtCNGC2 also differ from the corresponding residues presumed to form the selectivity filters of all other plant cngcs identified to date (i.e. the 20 Arabidopsis sequences, the two known tobacco [*Nicotiana tabacum*] sequences, and the barley [*Hordeum vulgare*] clone; Maser et al., 2001; also see Figure 2).

Further evidence supporting the strong discrimination against Na^+ conduction by AtCNGC2 is presented in Figure 3. AtCNGC2 currents were studied using a second heterologous expression system, i.e. HEK 293 cells. We previously have used Fura-2 flourescence measurements to document Ca^{2+} uptake by HEK cells expressing AtCNGC2 (Leng et al., 1999). Results presented in Figure 3 provide documentation that HEK cells are another appropriate system for voltage clamp analysis of a plant cngc, and that cells transfected with the AtCNGC2 cDNA show strong selectivity for K^+ over Na^+ conductance. cAMP-dependent AtCNGC2 K^+ currents were found to be inwardly rectified (Fig. 3A) and noninactivating (see Fig. 3A insert). Selectivity for K^+ over Na^+ conductance by AtCNGC2 appears to be stronger when measured using HEK cells as an expression system than we measure using oocytes (Fig. 1). There was no significant difference in conductance of Na^+ by HEK cells transfected with the AtCNGC2 cDNA in the absence (i.e. leak currents) or presence of cAMP (Fig. 3A), or between HEK cells expressing AtCNGC2 and those transfected with just the CD-8 plasmid (i.e. endogenous HEK currents) in the presence of cAMP ($n = 6$ in all cases; data not shown). A more detailed analysis of Na^+ currents from these experiments is presented in Figure 3B. Representative time-dependent Na^+ currents recorded from HEK cells transfected with the AtCNGC2 cDNA, or just the CD-8 plasmid ("endogenous currents"), are shown in Figure 3B with an expanded current scale. There appears to be an endogenous, fast-inactivating inward current that can be recorded from native HEK membranes (right side of Fig. 3B) that may increase slightly in the presence of cAMP. Recordings from a cell transfected with the AtCNGC2 cDNA are similar in the presence or absence of perfusion bath dibutyryl-cAMP (left side of Fig. 3B). Thus, we conclude that AtCNGC2 is the first cloned (from either
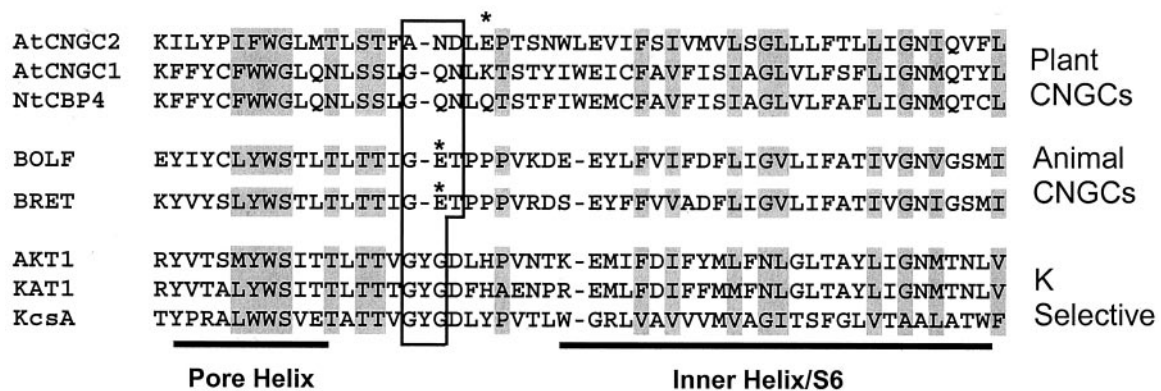
Figure 2. Amino acid sequence in and near the pore region of K^+-selective channels and cyclic nucleotide-gated channels. The plant cngcs used in the experiments described in this report are shown, along with the bovine retinal (BRET) and olfactory (BOLF) cngcs (accession nos. X51604 and X55010, respectively), the plant K^+ channels AKT1 and KAT1 (accession nos. X62907 and U25088, respectively), and the K^+ channel KcsA (accession no. Z37969) are included in this alignment. The pore helix and selectivity filter of the pore region, along with the flanking helix of the S6 (or "inner helix" in the case of KcsA) membrane-spanning region of the channels are shown. The selectivity filter of the K^+ channels and corresponding amino acids of the cngcs are boxed. The Glu residue (within the selectivity filter) responsible for external Ca^{2+} block of animal cngcs (see text) is denoted with an asterisk, as is the Glu near this position in the pore region of AtCNGC2. Amino acid sequence similarity shared by the channels included in this alignment analysis is denoted by shading.

A

B
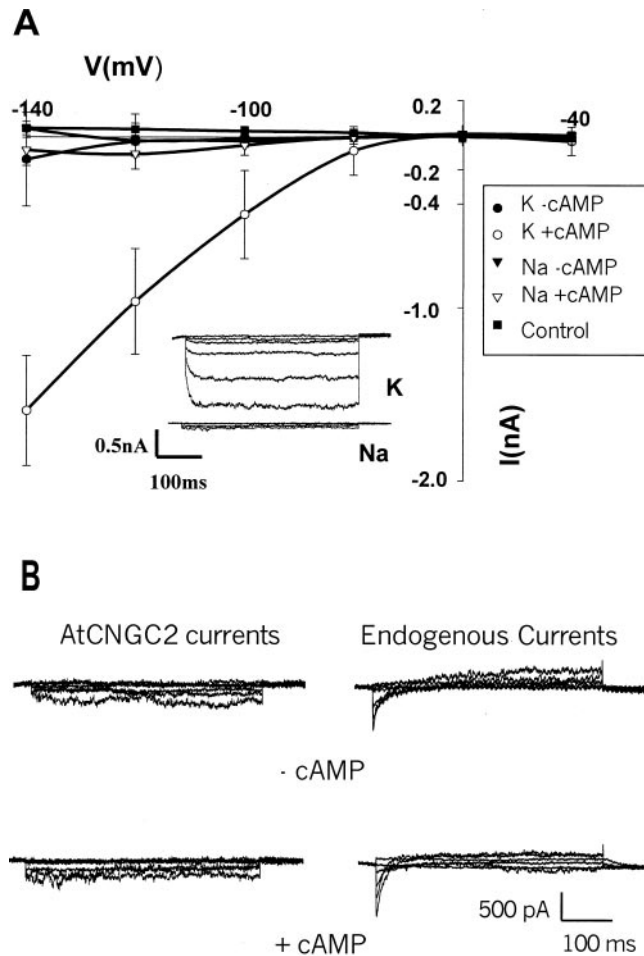
Figure 3. Current-voltage relationship of AtCNGC2 currents recorded from HEK cells (whole-cell configuration) with 145 mM K+ or Na+ in the perfusion bath, in the presence and absence of dibutyryl-cAMP. Command voltages were applied in 20-mV steps between −40 and −140 mV. The currents recorded in the presence of cAMP are presented in this figure without leak subtraction, i.e. separate current values are shown for K+ or Na+ in the presence and absence of cAMP. The control treatment shown in Figure 3A is the K+ current measured from HEK cells that were not transfected with AtCNGC2 recorded in the presence of cAMP. A, Current/voltage relation generated under the varying treatments at a range of command voltages; results are presented as means ($n = 6$) ± SE. The insert shows representative time-dependent currents for HEK cells expressing AtCNGC2 in the presence of cAMP and either K+ or Na+ in the bath solution. B, Time-dependent Na+ currents presented with an expanded scale. Representative currents are shown for HEK cells that were not transfected with the AtCNGC2 cDNA (endogenous currents) and for cells expressing AtCNGC2 in the presence and absence of dibutyryl-cAMP.

plants or animals) K+-conducting ion channel (of any family) that displays strong selectivity against Na+ without the presence of the "GYG" triplet in the selectivity filter of the pore domain.

Channel Characterization

Cyclic nucleotide-gated channels are defined functionally as ligand-gated channels that are activated

by ligand (cAMP or cGMP) binding to the channel protein. Conductance facilitated by some plant (Hoshi, 1995) and animal (Bruggemann et al., 1993) voltage-gated K+ channels is also affected by cyclic nucleotides, but in a different manner. In this case, the rectified conductance of channels is activated by voltage, but direct binding of cyclic nucleotide to the protein modulates the voltage-current relationship. The K+-selective, voltage-gated channels KAT1, AKT1, and KST1, plant homologs of animal ("Shaker") K+ channels, have cyclic nucleotide-binding sites (Anderson et al., 1992; Sentenac et al., 1992; Mueller-Roeber et al., 1995), as is the case with AtCNGC2. However, these channels are structurally and functionally distinct from cngcs. Binding of cyclic nucleotide to this class of plant channels results in a reduction of current at a given voltage, but voltage is the primary determinant of conductance (Hoshi, 1995). Cytosolic cyclic nucleotides are also known to modulate the conductance of other classes of K+-selective channels, but in an indirect fashion (Zagotta and Siegelbaum, 1996), through cyclic nucleotide-dependent protein kinase phosphorylation of the channel, which alters channel conductance (Wang and Giebisch, 1991; Rudy et al., 1991). K+ currents across some native plant cell membranes are, in fact, modulated by cAMP-dependent protein kinase phosphorylation of the channel (Li et al., 1994).

Further evidence that AtCNGC2 is a plant cngc is presented in Figure 4. We have demonstrated thus far (Figs. 1 and 3; also see Leng et al., 1999) that when a lipophilic analog (dibutyryl-cAMP or cGMP) of a cyclic nucleotide is added to the perfusion bath, whole-cell recordings of HEK cells or two-electrode voltage clamp recordings from intact oocytes expressing the AtCNGC2 coding sequence showed increased amplitude of inward K+ currents. In these experiments, the possibility that cyclic nucleotide activation of the channel is indirect (e.g. via channel phosphorylation mediated by a cyclic nucleotide-dependent kinase) cannot be discounted. The experiments shown in Figure 4 address this possibility. These recordings were made from (inside-out) patches pulled from oocytes injected with AtCNGC2 cRNA. In this configuration, the lipophilic form of the cyclic nucleotide is not required for activation; cAMP added to the perfusion bath can reach the cyclic nucleotide binding site of the channel without diffusing through the cell membrane. Because these recordings are made from membrane patches, the cytosolic contents of the cell are absent; therefore, the effect of cAMP on the channel cannot be attributed to cytosolic signaling systems such as kinase-dependent phosphorylation. When a membrane patch is clamped at 0 mV, and then exposed to a 60-mV step potential in the absence of cAMP, no channel currents are evoked (Fig. 4A). When the same membrane patch is exposed to the 60-mV step potential while cAMP is present in the perfusion bath solution, K+
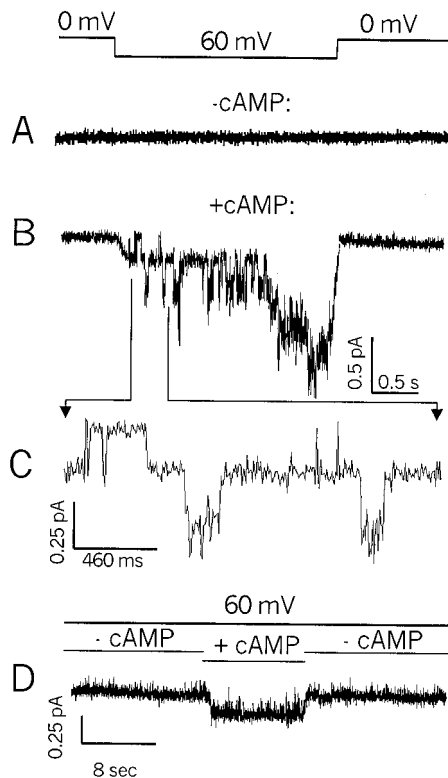
Figure 4. K$^+$ currents recorded (inside-out patch configuration) in the presence and absence of cAMP from membranes of oocytes expressing AtCNGC2. Currents shown in A and B are from the same patch. The bar at the top indicates the patch was held at 0 mV, and a 60-mV step voltage was applied as indicated for the recordings shown in A and B. Currents shown in A were obtained in the absence of cAMP, and the recording shown in B is from the same patch after perfusion with bath solution containing cAMP. The current tracing in C is a portion of the recording in B presented with an expanded scale. The current tracing in D is from a different patch, which was held at 60-mV command potential during the time course of the recording. The bars above the current trace indicate time periods when cAMP was absent, or applied to the bath solution.

currents are evident (Fig. 4B). A portion of the recording shown in Figure 4B is shown in an expanded scale in Figure 4C. The expanded scale presentation in Figure 4C shows several discreet channel-opening events; the current evoked by application of cAMP to the patch was generated from the opening of four to five individual channels during the time period shown in Figure 4B. Determination of single channel conductance of an ion channel is properly undertaken by evaluation of current amplitude histograms of single channel currents recorded from membrane patches clamped at a range of voltages. The experiments shown in Figure 4 were undertaken at a single current-evoking voltage (i.e. 60 mV). Therefore, we can only determine a preliminary estimation of AtCNGC2 single channel conductance from these data. The single channel conductance of AtCNGC2 calculated from the data presented in Figure 4 is approx-

imately 4 pS (-60 mV, 130 mM K$^+$). This estimated single channel conductance is substantially lower than that measured for animal cngcs (approximately 20–25 pS, see Torre and Menini, 1994; Lee et al., 2001).

AtCNGC2 current recordings obtained from another oocyte membrane patch are shown in Figure 4D. In this case, a 60-mV potential gradient was imposed across the membrane during the entire time course. During this time course (as indicated), cAMP was applied to the patch, and then the patch was again perfused with bath solution lacking cAMP. In this case, current was generated across the patch only during the application of cAMP. The results shown in Figure 4, therefore, provide evidence consistent with the presence of cngcs in the membrane of oocytes injected with AtCNGC2 cRNA. Currents were evoked by the application of cAMP in the absence of the cytosolic factors, which could be present within the intact cell (HEK or oocyte). These data support the contention that cAMP activation of AtCNGC2 currents is a direct effect of the ligand binding to the channel.

Another common attribute of (most) cyclic nucleotide-gated channels in animal membranes is that they both conduct, and are blocked by Ca$^+$ external to the cell (Biel et al., 1999a). A single Glu residue within the selectivity filter (see Fig. 2) has been shown to be involved in the Ca$^+$ block; mutation of this Glu to a neutral residue reduces sensitivity of cngcs such as the bovine rod channel (CNG1) to extracellular Ca$^+$ by two orders of magnitude (Root and MacKinnon, 1993; Eismann et al., 1994). The pore of AtCNGC2 contains a Glu residue (E419), whereas many of the other Arabidopsis cngcs do not (Köhler et al., 1999; Maser et al., 2001; also see Fig. 2). Prior work from this laboratory (Leng et al., 1999) has demonstrated Ca^{2+} conductance by AtCNGC2. Results presented in Figure 5 demonstrate that, in addition to being permeable to Ca^{2+}, AtCNGC2 currents are blocked by external Ca^{2+}. When bath [Ca^{2+}] is increased from 1.8 to 9 mM (bath [K$^+$] was 96 mM in both cases), total current through AtCNGC2 is reduced.

Block by external Ca^{2+} of animal cngcs has been shown to be voltage dependent, and therefore contributes to rectification of these channels (Eismann et al., 1994; Seifert et al., 1999). Effects of external Ca^{2+} on this family of channels is thought to be one factor that contributes to their physiological role in different cell types of animals (Zagotta and Siegelbaum, 1996). In this context, it is interesting to note that the external block of AtCNGC2 currents at high external Ca^{2+} was associated with a shift in the reversal potential to a more negative value (Fig. 5A). Tail current analysis (tail currents are evident in the representative time-dependent recordings shown in Fig. 5B) of the data presented in Figure 5 indicate that the reversal potential at 1.8 mM bath Ca^{2+} (-54 ± 11 mV;

A
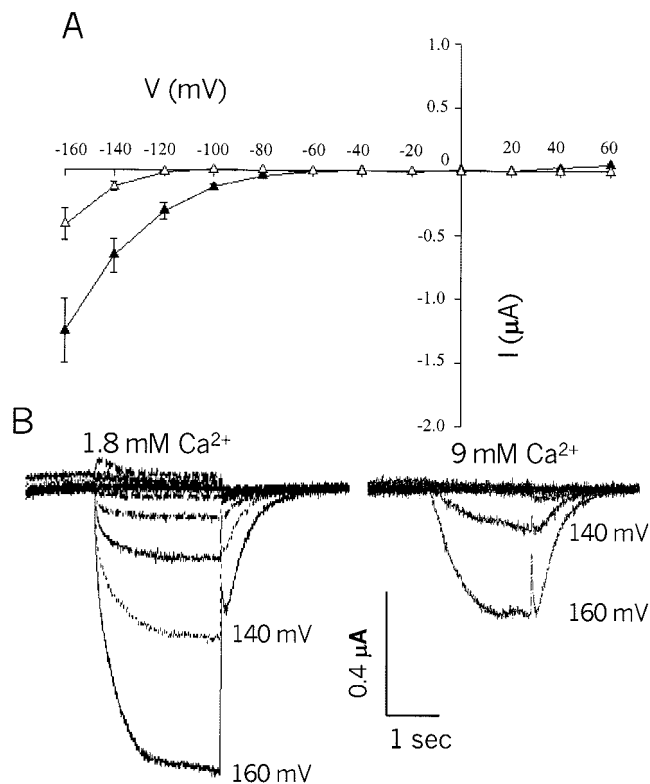
Figure 5. Calcium inhibition of (leak-subtracted) K^+ currents recorded in the two-electrode configuration from oocytes expressing AtCNGC2. Command voltages were applied in 20-mV steps between +60 and −160 mV. A, Leak-subtracted AtCNGC2 currents recorded from oocytes in the presence of 96 mM K^+ and either the standard (1.8 mM) Ca^{2+} (black symbols) or high (9 mM) Ca^{2+} (white symbols) in the perfusion bath. Data are presented as means ($n = 7$ for 1.8 mM Ca^{2+}; $n = 6$ for 9 mM Ca^{2+}) ± SE. B, Representative time-dependent AtCNGC2 currents recorded in the presence of high or low perfusion bath Ca^{2+}.

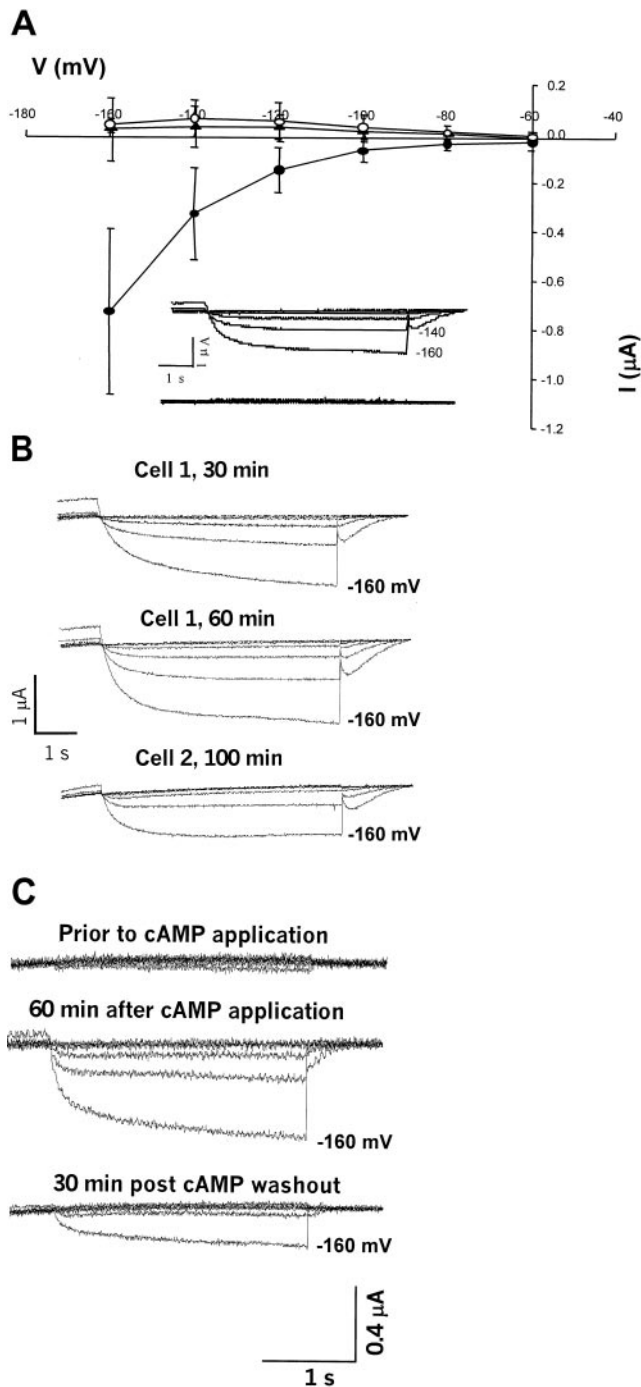$n = 7$) shifted to −92 ± 13 mV ($n = 6$) at 9 mM Ca^{2+}. This shift in reversal potential at high external Ca^{2+} may be because of a voltage dependence of the Ca^{2+} block of AtCNGC2 currents. Increasing external $[Ca^{2+}]$ has also been shown to shift the reversal potential of (current carried by K^+ and Ca^{2+}) a cloned animal cngc expressed in oocytes (Eismann et al., 1994). The block by external Ca^{2+} appears to be associated with an increase in the time constant for channel activation (Fig. 5B). Increasing bath $[Ca^{2+}]$ to 9 mM increased the half time for channel activation (τ); in the experiment shown in Figure 5, τ increased from 119 ± 14 ms ($n = 7$) at low bath Ca^{2+}, to 333 ± 23 ms ($n = 6$) at high bath Ca^{2+}. The presence of a Glu in the pore region of AtCNGC2 that is not present in the pore of AtCNGC1 and NtCBP4 (Fig. 2) and other plant cngcs (Köhler et al., 1999; Maser et al., 2001) raises the intriguing possibility that external Ca^{2+} may affect plant cngcs differently; keeping one channel (i.e. AtCNGC2) closed, whereas others remain open at some hyperpolarizing membrane potentials. This point will be the focus of our future studies.

Functional Expression of Other cngcs

α-Subunits (pore-forming) of voltage-gated inward-rectified, K^+-selective proteins with six membrane-spanning domains, a pore, and a voltage sensor ("Shaker" homologs) were the first ion channels to be cloned from plants (Anderson et al., 1992; Sentenac et al., 1992). Some members of this ion channel family were able to be functionally expressed in heterologous systems such as X. laevis oocytes, allowing for voltage clamp analysis of their channel properties (e.g. Schachtman et al., 1992; Mueller-Roeber et al., 1995), whereas others were more recalcitrant and failed to express in oocytes (Schachtman, 2000). It appears that this may be the case with plant cngcs. In our hands, AtCNGC2 has not readily expressed well in oocytes. Other researchers have communicated similar observations. The recalcitrance of AtCNGC2 expression (and expression of other plant cngcs) in oocytes may be caused by toxic effects of plant cngc expression on oocyte vitality. The following observations (in all cases, data not shown, or anecdotal observations) are consistent with this speculation. We have found that when the physiological vitality of oocytes is not optimal, expression of AtCNGC2 is compromised. Oocyte quality and frog growth conditions (adding salt to the frog tanks) are critical. When we see low (approximately 1–2 μA maximal) KAT1 currents (for example, during the summer months), we typically get no AtCNGC2 expression. Expression level of plant cngcs in oocytes is quite variable, and is often times much lower (and requires more days of incubation) than that obtained with either KAT1 or the animal cngc rCNGC1 (accession no. U48803; we used KAT1 and rCNGC1 routinely as controls). Oocytes injected with plant cngcs begin to die just after expression starts, whereas the same oocyte preparations injected with KAT1 or rCNGC1 stay healthy for weeks. The basis for this may be that plant cngcs may leak current during oocyte incubation, perhaps causing K^+ efflux or Ca^{2+} influx; either condition would be toxic over the many days of incubation. Oocyte mortality upon plant cngc expression may be reduced by replacing some of the incubation medium Na^+ with K^+, or by lowering the medium Ca^{2+} (adding the Ca^{2+} channel blocker l-cis-diltiazem or replacing one-half of the Na^+ with K^+ decreased mortality in one preliminary study). Induction of plant cngc currents in oocytes by application of lipophilic cyclic nucleotides sometimes can take either a very long time (relative to the routine analysis of voltage-gated channels such as KAT1), or possibly require higher than physiologically relevant levels of perfusion bath (cAMP). However, it should be noted that published reports of electrophysiological analysis of some animal cngcs (i.e. cloned

Leng et al.

A
V (mV)

B
Cell 1, 30 min

-160 mV

Cell 1, 60 min

-160 mV

Cell 2, 100 min

-160 mV

C
Prior to cAMP application

60 min after cAMP application

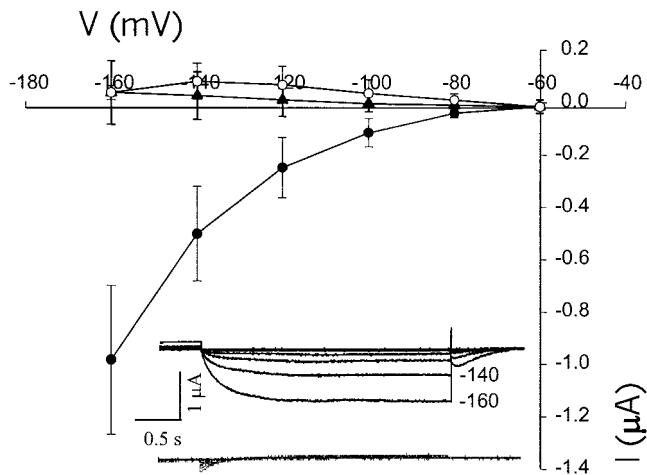-160 mV

30 min post cAMP washout

-160 mV

Figure 6. Electrophysiological characterization of a tobacco cyclic nucleotide-gated channel ("NtCBP4") expressed in oocytes. All recordings were made in the two-electrode configuration, and are presented without leak subtraction. Command voltages were applied in 20-mV steps between −60 and −160 mV. In all cases, [dibutyryl-cAMP] was 5 mM, and the standard oocyte bath solution was used (i.e. with 96 mM K$^+$). A, Current-voltage relationship of NtCBP4 currents. NtCBP4 showed no (inward) currents before addition of dibutyryl-cAMP to the perfusion bath solution (▲). After application of dibutyryl cAMP to the perfusion bath, currents were monitored over 20-min intervals (data not shown), and reached maximum values by (approximately) 60 min (●) in this experiment. Water-injected oocytes displayed no inward currents after exposure to

channels expressed in HEK cells or *X. laevis* oocytes) have also used millimolar or higher levels of cyclic nucleotides to study channel currents (e.g. Yao et al., 1995; Seifert et al., 1999; Crary et al., 2000; Rich et al., 2000). Our initial studies of AtCNGC2 expressed in HEK cells (e.g. Fig. 3; see also Leng et al., 1999) suggest that expression is less toxic to this heterologous system than oocytes. We have not yet evaluated the relative toxicity of other plant cngc channels in these heterologous expression systems.

The above information is provided for other researchers working with cloned plant cngcs, and as a context for the data presented in Figures 6 and 7. As mentioned above, recent studies have uncovered new roles of plant cngcs, perhaps beyond that of signal transduction. AtCNGC1, and a tobacco cngc, NtCBP4, may be involved in Ca^{2+} and/or K$^+$ uptake from the soil. In this role, they may provide a pathway for deleterious heavy metal (Pb^{2+}) or Na$^+$ uptake. Understanding the role plant cngcs play in plant growth and development could be aided by characterization of their molecular properties. Prior work from this lab (Leng et al., 1999) is the only published characterization to date of a plant cDNA (i.e. AtCNGC2) as a cyclic nucleotide-gated channel. Other cDNAs encoding protein homologs of AtCNGC2 have not been yet characterized as ligand-gated channels. Results presented in Figures 6 and 7 extend our electrophysiological analysis of plant cngcs to NtCBP4 and AtCNGC1. Our routine screens of plant cngc expression in oocytes have routinely failed to demonstrate expression of these channels. We have observed no inward K$^+$ currents in an oocyte expressing one (AtCNGC1) of these channels at low (100 μM) [cAMP], whereas increasing bath cAMP up to the mM range did induce currents in the same oocyte (data not shown). When higher perfusion bath cAMP concentrations are used (as compared with those used to evaluate AtCNGC2 currents), along with longer incubation times (postapplication of cyclic nucleotide), we have observed repeatable induction of inward K$^+$ currents in oocytes

dibutyryl-cAMP for 60 min (○). Results are presented as means (n = 4) ± SE. The insert shows representative time-dependent currents recorded from oocytes expressing NtCBP4 before (bottom of insert) and 60 min after addition of dibutyryl cAMP (top of insert). B, Increase of cAMP-activated NtCBP4 currents over time. Time-dependent current recordings are shown for two oocytes expressing NtCBP4. In one case (cell 1), current is shown to be greater at 60 min than that recorded after 30-min incubation in perfusion bath solution containing dibutyryl-cAMP. In the case of the second cell, noticeable currents were recorded only after 100 min incubation in dibutyryl-cAMP; these currents were substantially lower than those recorded from cell one, however. C, Reversal of cAMP activation of plant cngc currents. The top time-dependent currents were recorded from an oocyte expressing NtCBP4 before addition of dibutyryl-cAMP to the perfusion bath solution. The middle current recordings were made 60 min after exposure of the oocyte to dibutyryl-cAMP. Shortly after these currents were recorded, dibutyryl-cAMP was removed from the perfusion bath solution; the recordings at the bottom of the figure were made 30 min after removal of dibutyryl-cAMP.

Figure 7. Electrophysiological characterization of a putative Arabidopsis cyclic nucleotide-gated channel ("AtCNGC1") expressed in oocytes. Command voltages were applied in 20-mV steps between −60 and −160 mV. All recordings were made in the two-electrode configuration, and are presented without leak subtraction. In all cases, [dibutyryl-cAMP] was 5 mM, and the standard oocyte bath solution was used (i.e. with 96 mM K^+). AtCNGC1 showed no (inward) currents before addition of dibutyryl-cAMP to the perfusion bath solution (▲). Currents were evident 3 h after addition of dibutyryl-cAMP to the perfusion bath solution (●) in this experiment. Water-injected oocytes displayed no inward currents after exposure to dibutyryl-cAMP for 3 h (○). Results are presented as means ($n = 4$) ± SE. The insert shows representative time-dependent currents recorded from oocytes expressing AtCNGC1 before (bottom of insert) and 3 h after addition of dibutyryl cAMP (top of insert).

injected with NtCBP4 (Fig. 6) and AtCNGC1 (Fig. 7) cRNA. In both cases, currents through these plant cngcs are inward rectified and noninactivating (Figs. 6 and 7), as is the case with AtCNGC2 (Fig. 3). Currents were evoked from oocytes expressing NtCBP4 and AtCNGC1 after unusually long incubation times with relatively high concentrations of bath lipophilic cAMP. An example of these long induction times is shown in Figure 6B. In one case, currents increased in magnitude up to 1 h after application of cAMP; in another, currents were noted after 100 min. As is the case with AtCNGC2 (data not shown, but see also data in Fig. 4D for patch configuration analysis of AtCNGC2), currents through these channels are reversibly induced by exposure to cyclic nucleotide; removal of cAMP from the perfusion bath reversed the activation of NtCBP4 (Fig. 6C). Water-injected oocytes evoked no measurable current over the long incubation periods required to activate NtCBP4 and AtCNGC1 (Figs. 6A and 7). It should be noted that AtCNGC2 also requires substantial exposure times to (lipophilic) cAMP before current activation, when measured in either intact oocytes (Leng et al., 1999; also Figs. 1 and 5) or HEK cells (Fig. 3). However, in the patch configuration, current activation is immediate (Fig. 4). Nonetheless, the data presented in Figures 6 and 7 support the characterization of AtCNGC1 and NtCBP4 as plant cngcs. These channels

display similar properties as plant K^+-selective channels such as KAT1, and the plant cngc AtCNGC2, in that they are inward rectified, and show no inactivation over the time periods tested.

We have not evaluated AtCNGC1 or NtCBP4 for conductance of ions other than K^+, or examined the activation of these channels by a range of cyclic nucleotide concentrations. We have also not yet subcloned the corresponding cDNAs into plasmids appropriate for expression in HEK cells. It is clear that the electrophysiological analysis of cloned plant cngcs will be an important research objective for facilitating their functional characterization. The work presented in this report extends our prior studies (Leng et al., 1999) by expanding our understanding of AtCNGC2 channel properties, and by presenting the first functional analysis that characterizes homologous plant cDNAs as also encoding cyclic nucleotide-gated cation channels.

MATERIALS AND METHODS

Cloning and DNA Manipulation

GenBank accession numbers for the cDNAs encoding plant cngcs used in this study are: AF079872, NtCBP4; Y16327, AtCNGC1; and AF067798, AtCNGC2. The cDNA encoding the tobacco (*Nicotiana tobacum*) NtCBP4 gene (Arazi et al. 1999, 2000) was prepared for expression in *Xenopus laevis* oocytes as follows. The coding region was amplified by PCR using gene-specific sense and antisense oligonucleotide primers, and cloned into the *Eco*RI-*Xho*I sites of a pEXO expression vector (Lingueglia et al., 1993). Orientation and sequence of the cloned amplified fragment were verified by sequencing. Methylated, capped, runoff transcripts encoding sense cRNAs were generated from NtCBP4 (and the Arabidopsis cDNAs encoding AtCNGC1 and AtCNGC2) using the Epicentre AmpliScribe Transcription Kit (Epicentre Technologies, Madison, WI). NtCBP4 cRNA was prepared using T7 RNA polymerase from *Not*I digested pEXO-NtCBP4 plasmid DNA. The resultant purified sample was used directly for injection into oocytes (50 nL per oocyte containing 50 ng cRNA). Similar amounts of the other cRNAs (prepared using the same transcription kit) were also injected into oocytes. A cDNA encoding the full-length AtCNGC1 coding sequence was prepared as follows. The coding region representing AtCNGC1 was amplified via PCR using an Arabidopsis single-stranded cDNA library (Library-in-a-Tube, Bio 101, Vista, CA) and upstream (containing an *Eco*RI site at 5′ end) and downstream (containing a *Not*I site at 5′ end) primers spanning the start and stop codons. The reaction was performed as described by the vendor. The resultant PCR product was digested with *Eco*RI and *Not*I and directionally subcloned into *Eco*RI-*Not*I-digested pBluescript II SK$^+$ (Stratagene, La Jolla, CA). The construct is labeled pBS-AtCNGC1. AtCNGC1 cRNA was synthesized from *Xba*I-digested pBS-AtCNGC1 essentially as described above. Protein encoded by the AtCNGC2 cDNA was expressed in oocytes as described previously (Leng et al., 1999), except that the coding sequence was

excised from the pZL plasmid and ligated into pGEM-HE. The pGEM-HE plasmid contains untranslated regions of the endogenous β-globulin protein of oocytes flanking the insertion site; the cRNA generated from this plasmid will contain the β-globulin untranslated regions, enhancing expression of the recombinant protein in oocytes (Liman et al., 1992). The AtCNGC2 coding sequence was prepared for expression in HEK cells by subcloning into the mammalian expression vector pcDNA3.1 (Invitrogen, Carlsbad, CA); after excision from the pZL construct, the AtCNGC2 coding sequence was ligated into the *Kpn*I and *Xba*I restriction sites of the pcDNA3.1 plasmid. Unless otherwise noted, standard molecular biology procedures were performed for all DNA and RNA manipulations (Ausubel et al., 1987). All plasmids were verified by sequencing before utilization in any experimental procedure.

Expression in HEK Cells

AtCNGC2 cDNA described above was expressed in the human embryonic kidney cell line HEK 293 (American Type Culture Collection, Rockville, MD) for voltage clamp measurements following methods modified from that of Immke et al. (1998). HEK cells were cultured in a CO_2 (5%) incubator (Napco, Winchester, VA) at 37°C in maintenance medium (Dulbecco's modified eagle medium [Gibco BRL, Grand Island, NY] with 10% [w/v] fetal bovine serum [Gibco] and 1% [w/v] penicillin/streptomycin added). HEK cells were cotransfected with the pcDNA3.1 plasmid (20 μg/0.2 mL) containing the AtCNGC2 coding sequence, and a plasmid encoding the CD8 antigen (1 μg/0.2 mL) by electroporation (Gene Pulser 2 electroporator, Bio-Rad, Hercules, CA) at 75 μF and 366 V. After electroporation, cells were plated on protamine (1 mg mL^{-1})-coated glass cover slips submerged in maintenance medium and incubated for 1 to 2 d before use for electrophysiological studies. On the day of recording, cells were washed with maintenance medium and incubated with M450 Dynabeads conjugated with anti-CD8 antibody at 1 μL/2 mL (Dynal, Oslo). Successful transfection was ascertained by the adherence of Dynabeads to a cell (Jurman et al., 1994). These cells were used for electrophysiological recordings in the whole-cell configuration at room temperature. Recordings were made with electrodes made from N51A glass pipettes (Garner Glass Co., Claremont, CA), which were pulled on a P87 instrument (Sutter, Novato, CA) and fire polished using an MF83 heater (Narishige, East Meadow, NY). Perfusion bath and pipette solutions were modified from those Rich et al. (2000) used for whole-cell voltage clamp analysis of the olfactory cngc upon expression in HEK cells. Bath solution contained 145 mM KCl (or NaCl as noted); 10 mM HEPES [4-(2-hydroxyethyl)-1-piperazineethanesulfonic acid]-KOH (or NaOH when appropriate), pH 7.4; 10 mM D-Glc, and 0.1 mM $MgCl_2$. Pipettes were filled with 145 mM N-methyl-D-glucamine; 10 mM HEPES-KOH, pH 7.4; and 0.5 mM $MgCl_2$. Cells were perfused with bath solution containing 100 μM dibutyryl-cAMP to activate channel currents. Voltage stimuli were generated and currents were recorded using pClamp 8.04 software (Axon Instruments,

Foster City, CA), an Axopatch 200B amplifier (Axon), and a Digidata 1320 analog/digital interface (Axon). Currents were filtered at 1 kHz and a -60-mV holding potential was used for all recordings. Data were analyzed with the Clampfit component of pClamp and plotted using Sigma Plot 3.0 software (SPSS Scientific, Chicago). Results are presented as means $\pm$ SE.

Expression in Oocytes

Whole-cell and patch recordings were made of plant cngcs after expression in *X. laevis* oocytes. Frog culture, oocyte preparation, and channel expression in oocytes was as described previously (Leng et al., 1999), except that 1 mL volume L^{-1} of course sea salt and 0.25 mL L^{-1} of Stress Coat (Aquarium Pharmaceuticals, Chalfont, PA) were added to the water in frog tanks. Current recordings in the two-electrode configuration were obtained with a GeneClamp 500 amplifier (Axon) and 1320 analog/digital interface, and filtered at 2 kHz. The pipette and perfusion bath solutions used for recording cngc currents have been used previously to study KAT1 currents (Schachtman et al., 1992) and AtCNGC2 currents (Leng et al., 1999) upon expression in oocytes. Pipettes were pulled from KIMAX-51 capillaries (KIMBLE Products, Vineland, NJ) and filled with 3 M KCl for use as electrodes. The bath solution contained 96 mM KCl (or 96 mM chloride salts of other monovalent cations), 1.8 mM $CaCl_2$, 1.8 mM $MgCl_2$, and 10 mM HEPES-KOH (NaOH, LiOH, or CsOH as appropriate, except N-methyl-D-glucamine was used in the case of Rb$^+$), pH 7.5, unless otherwise noted. The bath solution was perfused at 2 mL min^{-1} into the 1-mL oocyte chamber. Holding potential for two-electrode recordings was -60 mV in all cases, and currents were evoked by adding 100 μM (or other concentrations as noted) of a lipophilic analog of cAMP (dibutyryl-cAMP) to the perfusion bath solution. cngc currents typically were recorded in the two-electrode configuration from whole oocytes just before, and then after exposure of the oocyte to (lipophilic) cAMP for approximately 40 min; in some cases (as noted), exposure times were longer. In some experiments, AtCNGC2 currents were recorded from inside-out membrane patches pulled from oocytes. In this case, the bath and pipette solutions contained 130 mM KCl, 0.2 mM EDTA, and 2 mM HEPES-KOH, pH 7.2. For patch recordings, voltage stimuli were generated and currents were recorded using pClamp 8.04 software, an Axopatch 200B amplifier, and a Digidata 1320 analog/digital interface. Currents were evoked by adding 100 μM cAMP to the bath solution with a gravity-driven, multibarrel perfusion system. In all cases, reagents and chemicals were purchased from Sigma Chemical Co. (St. Louis), unless otherwise noted. Upon request, all novel materials described in this publication will be made available in a timely manner for noncommercial research purposes, subject to the requisite permission from any third-party owners of all or parts of the material. Obtaining any permissions will be the responsibility of the requestor.

ACKNOWLEDGMENTS

LITERATURE CITED

Anderson JA, Huprikar SS, Kochian LV, Lucas WJ, Gaber RF (1992) Functional expression of a probable *Arabidopsis thaliana* potassium channel in *Saccharomyces cerevisiae*. Proc Natl Acad Sci USA **89:** 3736–3740

Arazi T, Kaplan B, Fromm H (2000) A high-affinity calmodulin-binding site in a tobacco plasma-membrane channel protein coincides with a characteristic element of cyclic nucleotide-binding domains. Plant Mol Biol **42:** 591–601

Arazi T, Sunkar R, Kaplan B, Fromm H (1999) A tobacco plasma membrane calmodulin-binding transporter confers Ni^{2+} tolerance and Pb^{2+} hypersensitivity in transgenic plants. Plant J **20:** 171–182

Ausubel FM, Brent R, Kingston RE, Moore DD, Seidman JG, Smith JA, Struhl K (1987) Current Protocols in Molecular Biology. John Wiley and Sons, NY

Biel M, Zong X, Hofmann F (1999a) Cyclic nucleotide gated channels. Adv Second Messenger Phsophoprotein Res **33:** 231–250

Biel M, Zong X, Ludwig A. Sautter A, Hofmann F (1999b) Structure and function of cyclic nucleotide-gated channels. Rev Physiol Biochem Pharmacol **135:** 151–171

Bruggemann A, Pardo LA, Stuhmer W, Pongs O (1993) Ether-a-go-go encodes a voltage-gated channel permeable to K$^+$ and Ca^{2+} and modulated by cAMP. Nature **365:** 445–448

Clough SJ, Fengler KA, Yu I-C, Lippok B, Smith RK Jr, Bent AF (2000) The *Arabidopsis dnd1* "defense, no death" gene encodes a mutated cyclic nucleotide-gated ion channel. Proc Natl Acad Sci USA **97:** 9323–9328

Crary JI, Dean DM, Maroof F, Zimmerman AL (2000) Mutation of a single residue in the S2–S3 loop of CNG channels alters the gating properties and sensitivity to inhibitors. J Gen Physiol **116:** 769–779

Doyle DA, Cabral JM, Pfuetzner RA, Kuo A, Gulbis JM, Cohen SL, Chait BT, MacKinnon R (1998) The structure of the potassium channel: molecular basis of K conduction and selectivity. Science **280:** 69–76

Eismann E, Muller F, Heinemann SH, Kaupp UB (1994) A single negative charge within the pore region of a cGMP-gated channel controls rectification, Ca2+ blockage, and ionic selectivity. Proc Natl Acad Sci USA **91:** 1109–1113

Finn JT, Grunwald ME, Yau KW (1996) Cyclic nucleotide-gated ion channels: an extended family with diverse functions. Annu Rev Physiol **58:** 395–426

Heginbotham L, Lu Z, Abramson T, MacKinnon R (1994) Mutations in the K$^+$ channel signature sequence. Biophys J **66:** 1061–1067

Hoshi T (1995) Regulation of voltage dependence of the KAT1 channel by intracellular factors. J Gen Phyisol **105:** 309–328

Immke D, Kiss L, Loturco J, Korn SJ (1998) Influence of non-P region domains on selectivity filter properties in voltage-gated K$^+$ channels. Receptors Channels **6:** 179–188

Jurman ME, Boland LM, Liu Y, Yellen G (1994) Visual identification of individual transfected cells for electrophysiology using antibody-coated beads. Biotechniques **17:** 876–881

Köhler C, Merkle T, Neuhaus G (1999) Characterization of a novel gene family of putative cyclic nucleotide- and calmodulin-regulated ion channels in *Arabidopsis thaliana*. Plant J **18:** 97–104

Köhler C Merkle T, Roby D, Neuhaus G (2001) Developmentally regulated expression of a cyclic nucleotide-gated ion channel from Arabidopsis indicates its involvement in programmed cell death. Planta **213:** 327–332

Köhler C, Neuhaus G (2000). Characterization of calmodulin binding to cyclic nucleotide-gated ion channels from *Arabidopsis thaliana*. FEBS Lett **471:** 133–136

Lang R, Lee G, Liu W, Tian S, Rafi H, Orias M, Segal AS, Desir GV (2000) KCNA10: a novel ion channel functionally related to both voltage-gated potassium and CNG cation channels. Am J Physiol Renal Physiol **278:** F1013–F1021

Lacombe B, Becker D, Hedrich R, DeSalle R, Hollmann M, Kwak JM, Schroeder JI, Le Novere N, Nam HG, Spalding EP et al. (2001) The identity of plant glutamate receptors. Science **292:** 1486–1487

Lee ML, Park YS, Kim W, Park C-S (2001) Electrophysiological characteristics of rat gustatory cyclic nucleotide-gated channel expressed in *Xenopus* oocytes. J Neurophysiol **85:** 2335–2349

Leng Q, Mercier RW, Yao W, Berkowitz GA (1999) Cloning and first functional characterization of a plant cyclic nucleotide-gated cation channel. Plant Physiol **121:** 753–761

Li W, Luan S, Schreiber SL, Assmann SM (1994) Cyclic AMP stimulates K$^+$ channel activity in mesophyll cells of *Vicia faba* L. Plant Physiol **106:** 957–961

Liman ER, Tytgat J, Hess P (1992) Subunit stoichiometry of a mammalian K+ channel determine construction of multimeric cDNAs. Neuron **9:** 861–871

Lingueglia E, Voilley N, Waldmann R, Lazdunski M, Barbry P (1993) Expression cloning of an epithelial amiloride-sensitive Na+ channel: a new channel type with homologies to *Caenorhabditis elegans* degenerins. FEBS Lett **318:** 95–99

Maathuis FJM, Sanders D (2001) Sodium uptake in *Arabidopsis thaliana* roots is regulated by cyclic nucleotides. Plant Physiol **127**: 1788–1797

Maser P, Thomine S, Schroeder JI, Ward JM, Hirschi K, Sze H, Talke IN, Amtmann A, Maathuis FJM, Sanders D et al. (2001) Phylogenetic relationships within cation transporter families of Arabidopsis. Plant Physiol **126**: 1646–1667

Mueller-Roeber B, Ellenberg J, Provart N, Willmitzer L, Busch H, Becker D, Dietrich P, Hoth S, Hedrich R (1995) Cloning and electrophysiological analysis of KST1, an inward rectifying K^+ channel expressed in potato guard cells. EMBO J **14**: 2409–2416

Rich TC, Fagan KA, Nakata H, Schaack J, Cooper DMF, Karpen JW (2000) Cyclic nucleotide-gated channels co-localize with adenylyl cyclase in regions of restricted cAMP diffusion. J Gen Physiol **116**: 147–161

Root MJ, MacKinnon R (1993) Identification of an external divalent cation-binding site in the pore of a cGMP-activated channel. Neuron **11**: 459–466

Rudy B, Kentros C, Vega-Saenz de Miera E (1991) Families of potassium channel genes in mammals: toward an understanding of the molecular basis of potassium channel diversity. Mol Cell Neurosci **2**: 89–102

Schachtman DP (2000) Molecular insights into the structure and function of plant K^+ transport mechanisms. Biochim Biophys Acta **1465**: 127–139

Schachtman DP, Schroeder JI, Lucas WJ, Anderson JA, Gaber RF (1992) Expression of an inward-rectifying potassium channel by the *Arabidopsis* KAT1 cDNA. Science **258**: 1654–1658

Schuurink RC, Shartzer SF, Fath A, Jones RL (1998) Characterization of a calmodulin-binding transporter from the plasma membrane of barley aleurone. Proc Natl Acad Sci USA **95**: 1944–1949

Seifert R, Eismann, Ludwig J, Baumann A, Kaupp UB (1999) Molecular determinants of a Ca^{2+}-binding site in the pore of cyclic nucleotide-gated channels: S5/S6 segments control affinity of intrapore glutamates. EMBO J **18**: 119–130

Sentenac H, Bonneaud N, Minet M, Lacroute F, Salmon J-M, Gaymard F, Grignon C (1992) Cloning and expression in yeast of a plant potassium ion transport system. Science **256**: 663–665

Sunkar R, Kaplan B, Bouche N, Arazi T, Dolev D, Talke IN, Maathuis FJM, Sanders D, Bouchez D, Fromm H (2000) Expression of a truncated tobacco *NtCBP4* channel in transgenic plants and disruption of the homologous Arabidopsis *CNGC1* gene confer PB^{2+} tolerance. Plant J **24**: 533–542

Torre V, Menini A (1994) Selectivity and single-channel properties of the cGMP-activated channel in amphibian retinal rods. *In* C Peracchia, ed, Handbook of Membrane Channels: Molecular and Cellular Physiology. Academic Press, New York, pp 345–358

Wang W, Giebisch G (1991) Dual modulation of renal ATP-sensitive K^+ channel by protein kinase A and C. Proc Natl Acad Sci USA **88**: 9722–9725

Weber W-M (1999) Ion currents of *Xenopus laevis* oocytes: state of the art. Biochim Biophy Acta **1421**: 213–233

White PJ (2001) The pathways of calcium movement to the xylem. J Exper Bot **52**: 891–899

Yao X, Segal AS, Welling P, Zhang X, McNicholas CM, Engel D, Boulpaep EL, Desir GV (1995) Primary structure and functional expression of a cGMP-gated potassium channel. Proc Natl Acad Sci USA **92**: 11711–11715

Zagotta WN, Siegelbaum SA (1996) Structure and function of cyclic nucleotide-gated channels. Annu Rev Neurosci **19**: 235–263